Fluorescence Photobleaching with Spatial Fourier Analysis: Measurement of Diffusion in Light-Scattering Media

D. A. Berk, F. Yuan, M. Leunig, and R. K. Jain

Department of Radiation Oncology, Massachusetts General Hospital, Harvard Medical School, Boston, Massachusetts 02114 USA

ABSTRACT A new method for the measurement of diffusion in thick samples is introduced, based upon the spatial Fourier analysis of Tsay and Jacobson (*Biophys. J.* 60:360–368, 1991) for the video image analysis of fluorescence recovery after photobleaching (FRAP). In this approach, the diffusion coefficient is calculated from the decay of Fourier transform coefficients in successive fluorescence images. Previously, the application of FRAP in thick samples has been confounded by the optical effects of out-of-focus light and scattering and absorption by the sample. The theory of image formation is invoked to show that the decay rate is the same for both the observed fluorescence intensity and the true concentration distribution in the tissue. The method was tested in a series of macromolecular diffusion measurements in aqueous solution, in agarose gel, and in simulated tissue consisting of tumor cells (45% v/v) and blood cells (5% v/v) in an agarose gel. For a range of fluorescently labeled proteins (MW = 14 to 600 kD) and dextrans (MW = 4.4 to 147.8 kD), the diffusion coefficients in aqueous solution were comparable to previously published values. A comparison of the spatial Fourier analysis with a conventional direct photometric method revealed that even for the weakly scattering agarose sample, the conventional method gives a result that is inaccurate and dependent on sample thickness whereas the diffusion coefficient calculated by the spatial Fourier method agreed with published values and was independent of sample thickness. The diffusion coefficient of albumin in the simulated tissue samples, as determined by the spatial Fourier analysis, varied slightly with sample thickness. In contrast, when the same video images were analyzed by direct photometric analysis, the calculated diffusion coefficients were grossly inaccurate and highly dependent on sample thickness. No simple correction could be devised to ensure the accuracy of the direct photometric method of analysis. These in vitro experiments demonstrate the advantage of our new analysis for obtaining an accurate measure of the local diffusion coefficient in microscopic samples that are thick (thickness greater than the microscope depth of focus) and scatter light.

GLOSSARY

a	dimensionless size of fluorescence measurement region for use with DPA
B	depth of bleach (Appendix)
c and C	local concentration of fluorophore (c) and its spatial Fourier transform (C)
D	diffusion coefficient ($cm^2\ s^{-1}$)
d_f	focal length of objective (Appendix)
f_c	spatial frequency resolution limit of objective (Appendix)
i and I	local intensity of the image (i) and the spatial Fourier transform (I)
I_0	value of the Fourier coefficient at time $t = 0$
L	sample thickness (μm)
q	magnitude of the spatial frequency (μm^{-1}), $q^2 = u^2 + v^2$
R_w	radius of the intensity measurement region for direct photometric analysis
R_0	Gaussian radius of the photobleached spot
u, v	spatial frequencies in the x and y directions (μm^{-1})
w	maximum optical path length error (Appendix)
Δz	defocus distance of object from the focal plane (μm)

Received for publication 17 March 1993 and in final form 9 September 1993.

Abbreviations used: BSA, F-BSA, bovine serum albumin and fluorescein-labeled BSA; DPA, direct photometric analysis (of FRAP video images); FITC, fluorescein isothiocyanate; FRAP, fluorescence recovery after photobleaching; MW, molecular weight (weight-averaged in the case of polydisperse polymers); NA, numerical aperture of objective; OTF, optical transfer function; PSF, point spread function; SFA, spatial Fourier analysis of FRAP video images.

0006-3495/93/12/2428/09 $2.00

INTRODUCTION

The motion of molecules in the interstitial space of tissue is a phenomenon with important biophysical, physiological, and clinical implications. Transport of molecules by diffusion depends on the physicochemical properties of both the diffusing molecule and the medium (Laurent et al., 1963; Ogston et al., 1973); thus, an experimentally determined interstitial diffusion coefficient serves as a probe of tissue structure. The transport of molecules in the interstitial space is a crucial step in the delivery of blood-borne material to cells (Jain, 1987). Diffusion is the dominant mode of interstitial transport for small solutes, and when the driving force for convection is diminished, it may be the dominant or at least a significant mechanism for the transport of macromolecules as well (Jain and Baxter, 1988). The diffusion coefficients of large molecules are also of clinical importance because of the implications for delivery of genetically engineered macromolecules: hindered diffusion in the interstitial space of solid tumors presents a barrier to the delivery of high-molecular-weight diagnostic and therapeutic agents and thus limits their effectiveness (Jain, 1993).

Current experimental techniques have limited capabilities for noninvasive measurement of diffusion in small samples

of tissue (over distances less than 1 mm). Results obtained with invasive techniques (Maroudas, 1980) that may disturb the fluid balance and damage the gel structure in the tissue must be interpreted with caution, because the occurrence of edema could drastically alter the diffusion characteristics of the tissue. Several investigators (Nakamura and Wayland, 1975; Fox and Wayland, 1979; Nugent and Jain, 1984; Clauss and Jain, 1990) have attempted to minimize the perturbation of tissue by using quantitative fluorescence intravital microscopy to measure the diffusion of fluorescently labeled dextrans and proteins in thin tissue preparations (mesentary tissue or rabbit ear chamber). The diffusion coefficient was calculated based on the spatial distribution of fluorescence (relaxation of fluorescence gradient) as the labeled material extravasated and spread into the interstitium.

More recently, Chary and Jain (1989) adapted the method of fluorescence recovery after photobleaching (FRAP) to measure the diffusion of albumin in the rabbit ear chamber. The principles of FRAP have been described often since its introduction (Peters et al., 1974; Axelrod et al., 1976; Jacobson et al., 1976). The molecule of interest is labeled with a fluorescent tracer and then allowed to equilibrate in the sample. A portion of the sample is exposed briefly to intense illumination; this causes the local photobleaching of the fluorescent label and thus creates a fluorescence-depleted spot or pattern. The eradication of the pattern by diffusive transport is monitored and the diffusion coefficient is calculated from the rate at which a uniform fluorescence distribution is reestablished.

Two major advantages of the fluorescence photobleaching method are: (i) it allows multiple local measurements of diffusion in the region of a small photobleached spot (~40 μm diameter), and (ii) it is able to distinguish diffusive from convective transport. A major limitation of this method is the requirement that the sample must be thin (i.e., a sample with thickness comparable to the microscope depth of focus) and without strong light-scattering characteristics (Lanni et al., 1981). In this paper, we describe the optical problems causing this constraint, and we present a new implementation of FRAP with spatial Fourier analysis (SFA) that ameliorates this problem and allows the measurement of diffusion coefficient in thick tissue samples.

Regardless of the method used to quantify the fluorescence distribution, the calculation of the diffusion coefficient generally relies on the principle that the fluorescence intensity observed under the microscope is linearly related to the concentration of fluorescently labeled molecules. As we will show, the fluorescence intensity detected by conventional fluorescence microscopy of thick samples is not directly proportional to the concentration of fluorescent material, but the use of SFA nevertheless allows the accurate calculation of the diffusion coefficient.

A series of in vitro FRAP experiments was performed to validate this method of analysis. In order to simulate the optical characteristics encountered in tissue, we devised a light-scattering, light-absorbing medium consisting of a dense suspension of cells immobilized in agarose gel. A range of macromolecules (fluorescently labeled dextrans and proteins of various molecular weights) were placed in aqueous solution, agarose gel, and in the agarose/cell composite. Samples were placed in observation chambers of various thicknesses and subjected to the FRAP experiment in order to verify that the measurement of bulk diffusion coefficient is accurate and independent of sample thickness.

THEORY

It is generally recognized that a conventional fluorescence microscopy image is contaminated by out-of-focus light. The Appendix uses the theory of image formation (Castleman, 1979; Agard, 1984) to describe how the fluorescence image of a bleached spot is distorted and how the distortion will affect the measurement of diffusion coefficient in thick samples (>50 μm) using a conventional FRAP method (direct photometric analysis, or DPA (Jain et al., 1990)). The same theory is used in this section to show that SFA (Tsay and Jacobson, 1991) can reliably measure the diffusion coefficient despite this distortion. For use with thick samples, the major advantage of this technique is that it allows calculation of the diffusion coefficient without explicit knowledge of the optical distortion of the image. With this method, it is unnecessary to determine the true spot size or bleach depth. In addition, the solution to the diffusion equation is simplified in Fourier transform space and requires no assumptions regarding the initial distribution of fluorescence.

According to image formation theory, the optical system of the microscope can be considered a linear shift invariant system characterized by the point-spread function (PSF) that describes the image created when an ideal point source of light is viewed through the microscope (Castleman, 1979; Agard, 1984). The image distortion caused by the optical properties of the microscope lenses, and by the light absorption and scattering properties of the sample itself, can be represented by the PSF. An alternative form of this function is the optical transfer function (OTF), which is the Fourier transform of the PSF. The image created by any true object is the convolution of the concentration distribution with the microscope PSF. Here we assume that emitted fluorescence is proportional to local fluorophore concentration, i.e., that the concentration is not so high as to cause self-quenching. The PSF of a microscopic system can be derived theoretically (Hopkins, 1955; Stokseth, 1969) based on the numerical aperture, focal length and the extent of defocus of the objective, or it can be measured experimentally (Hiraoka et al., 1990).

During the FRAP experiment, the sample containing a uniform distribution of fluorescent molecules is briefly exposed to laser illumination at time $t = 0$. The concentration gradient along the optical axis, perpendicular to the x- and y-axes, is assumed to be negligible compared to gradients in the x-y plane so that a two dimensional diffusion equation describes the concentration redistribution in the bleached region governed by the diffusion coefficient D:

$$\partial c/\partial t = D\nabla^2 c \tag{1}$$

where $c(x, y, t)$ is the concentration relative to the pre-bleach distribution. If the concentration is then subjected to a two-dimensional Fourier transform (C) with respect to x and y, the solution to the transformed equation is a simple exponential decay:

$$C(u, v, t) = C(u, v, 0)\exp[-4\pi(u^2 + v^2)Dt] \quad (2)$$

where u and v are the spatial frequencies.

As discussed previously, the concentration is related to the observed image by the PSF. The changes in inner-filtering and reabsorption due to reduction in fluorophore concentration are neglected in this study (Tanke et al., 1982), thus the PSF is independent of time. In the Fourier transform space,

$$I(u, v, t) = C(u, v, t)\mathrm{OTF}(u, v) \quad (3)$$

where $I(u, v, t)$ is the fluorescence intensity (corrected for background fluorescence) and OTF is the optical transfer function mentioned previously. Therefore, the spatial transform of the image will obey the same exponential decay as the concentration profile:

$$I/I_o = C/C_o = \exp[-4\pi^2q^2Dt] \quad (4)$$

where $I_o = I(u, v, 0)$, $C_o = C(u, v, 0)$, and $q^2 = u^2 + v^2$.

By measuring the decay of the spatial Fourier transform, the diffusion coefficient can be calculated without determining the OTF of the microscope, and without determining the true concentration distribution in the sample.

MATERIALS AND METHODS

Fluorescein isothiocyanate (FITC) and FITC-labeled dextrans were obtained from Sigma (St. Louis, MO). The dextrans had weight-average molecular weights (MW) of 4,400, 18,900, 40,500, 69,000, and 147,800. Fluoresceinated bovine serum albumin (F-BSA, MW 68,000), lactalbumin (MW 14,000), IgG (MW 150,000), and cationized ferritin (MW 600,000) were obtained from Molecular Probes (Eugene, OR). Aqueous samples were prepared by dissolving the fluorescent material (0.5 g/liter) in phosphate-buffered saline. Gel samples were prepared by adding a concentrated fluorescent aqueous solution to a cooling 2% agarose (Sigma) solution (at 40°C) to obtain a final fluorophore concentration of 0.5 g/liter. Aqueous and liquid agarose solutions were drawn by capillary force into rectangular glass microslide chambers (Vitro Dynamics, Rockaway, NJ), and the ends of the chambers were blocked with a sealing compound (Hemato-seal, Fisher). The agarose samples were allowed to gel in the refrigerator (5°C) for 12 h before being brought back to room temperature for the experiments. All samples were allowed to equilibrate at room temperature (~24°C) before being placed on the microscope stage for measurement.

To simulate the light absorption and scattering encountered in tissue, a suspension of cancer cells and red blood cells in agarose gel was also prepared. One volume of packed mouse red blood cells was mixed with 9 volumes of packed human colon carcinoma (LS174T) cells and 1 volume of F-BSA solution (11 g/liter). This suspension was then mixed with 11 volumes of 2% liquid agarose solution at 40°C. The suspension was drawn into capillary microslides of 0.05-mm, 0.20-mm, and 0.40-mm thicknesses and allowed to cool in a refrigerator overnight.

The FRAP apparatus is similar to that described by Jain et al. (1990). The sample is placed on the stage of an upright microscope (Universal; Zeiss, Thornwood, NY) equipped for epi-illumination. The excitation filter (485 nm) and barrier filter (530 nm) were selected for use with fluorescein. By means of a beam splitting mirror, epi-illumination could be provided by both a conventional mercury arc lamp (100-W lamp, Osram, Munich; with stabilized power supply and convection-cooled housing, models 68806 and 60000, Oriel Corp., Stratford, CT) and by an argon laser (model 2020; Spectra Physics, Mountain View, CA). The laser was operated in the TEM_{00} mode (i.e., the intensity obeyed a radially symmetric Gaussian profile). The beam passed through a spatial filter (model 900; Newport, Fountain Valley, CA), through the microscope epi-illumination port and was focused on the back focal plane of the objective. With the 20×, N.A. 0.4 objective used for these experiments, the laser spot radius within the sample (the Gaussian radius of the attenuated beam projected onto a 50 μm thick layer of FITC solution) was 20 μm.

A sample of known thickness was placed on the microscope stage, and the objective was focused at the midpoint of the microslide depth. After a brief exposure to laser illumination (10 ms) the sample was observed under conventional epi-fluorescence illumination by means of an intensified CCD camera (model 2400; Hamamatsu, Japan). Fluorescence images were digitized directly (DT-2851 image processing board, Data Translation, Marlboro, MA; in an IBM PC-AT computer, Boca Raton, FL) and stored at a rate of 5 images/s. Only a portion (70 × 90 pixels) of the full 480 × 512 pixel image was stored for analysis. Although the illumination intensity varied somewhat over the field of view (~25% reduction at the edges relative to the center), the illumination within the image acquisition region was uniform (<5% variation). The fluorescence intensity in a region of the image far from the laser spot was also monitored to detect the occurrence of photobleaching by the conventional light source; no appreciable bleaching was detected. An image of a stage micrometer was acquired in order to establish the spatial sampling rates (vertical and horizontal distances between pixels). The pixel dimension was approximately 1 μm in both directions.

The fluorescence intensity was measured in a sample containing water but no fluorescein, and this background value was subtracted from each pixel of each acquired image. This correction was necessary for the direct photometric analysis, as it is important to subtract out any signal that is not produced by the labeled molecules. In the implementation of the spatial Fourier analysis, this correction was not essential, because the initial pre-bleach image was subtracted from each post-bleach image. A two-dimensional discrete Fourier transform was then performed on each differential image. The three Fourier coefficients corresponding to the lowest three spatial frequencies were then fit to Eq. 4 by means of a nonlinear least-squares (modified Levenberg-Marquardt) curve-fitting algorithm (Marquardt, 1963). The lowest frequencies were selected for the fit in order to maximize the signal-to-noise ratio and the temporal resolution. The low frequency components have the greatest magnitude in the initial post-bleach image, and they decay at the slowest rate. The three sets of components were simultaneously fit to Eq. 4, giving four independent parameters: D and the three separate initial values, I_0. The analyses were performed on a Sun 3 workstation (Sun Microsystems, Mountain View, CA), and used IMSL (Houston, TX) subroutines for two-dimensional discrete Fourier transforms and nonlinear least squares curve fitting.

The FRAP data were also analyzed by DPA similar to approaches described by Jain et al. (1990) and Kaufman and Jain (1991). For the initial post-bleach image, the spot center was determined and the intensity was fit to the form of a Gaussian curve similar to the profiles shown in the Appendix. This analysis of intensity distribution provided the bleach depth and spot radius. Then each image was examined to find the average fluorescence intensity in a circular region of radius 20 μm centered on the spot. The recovery of this intensity from the immediate post-bleach minimum to an intensity equal to the pre-bleach value was fit to the following equation:

$$\frac{F(0^-) - F(t)}{F(0^-) - F(0)} = \frac{1 - \exp(-2a^2/(1 + 8Dt/R_0^2))}{1 - \exp(-2a^2)}, \quad (5)$$

where $F(0^-)$ is the prebleach intensity and $a = R_w/R_0$, the ratio of the circular window radius to the Gaussian spot radius. This method could be termed "conventional" in the sense that it relies on the fluorescence intensity as a measure of local concentration, and it follows the principle introduced by Axelrod et al. (1976) and the method of analysis given by Yguerabide et al. (1982). Diffusion coefficients obtained by the SFA and DPA of the same images were evaluated statistically by analysis of variance and the unpaired t-test (performed by StatView 4.0, Abacus Concepts, Berkeley, CA, on a Macintosh computer, Apple, Cupertino, CA)

RESULTS

Determination of diffusion coefficient and the effect of molecule size

Fig. 1 shows the fluorescence recovery of F-BSA in water. In Fig. 1 *a*, the Fourier coefficients are plotted on a linear scale versus frequency-scaled time. The decay of each of the three components fits well to the same theoretical line. Fig. 1 *b* shows the data from Fig. 1 *a* plotted on a semilogarithmic scale to demonstrate that the bulk of the recovery is described by the single exponential decay. Fluorescence recoveries of free FITC and lactalbumin solutions are also shown in Fig. 1 *b*.

The diffusion coefficients measured in this study are in agreement with previously published values for the same molecules or molecules of similar molecular weight. The protein diffusion coefficients (mean ± SD) at 23°C were: for free FITC, $D = 26\ (\pm\ 4) \times 10^{-7}$ cm^2/s; for lactalbumin, $D = 9.6\ (\pm\ 0.4) \times 10^{-7}$ cm^2/s; for BSA, $D = 6.0\ (\pm\ 0.3) \times 10^{-7}$ cm^2/s; for IgG, $D = 4.0\ (\pm\ 0.5) \times 10^{-7}$ cm^2/s. Fig. 2 *a* summarizes the measured diffusion coefficients of the various proteins in aqueous solutions. For the purposes of comparison, the figure also shows diffusion coefficient values of various proteins, as measured by various investigators and summarized by Altman and Dittmer (1972). The diffusion coefficients calculated for the aqueous samples of dextran are plotted in Fig. 2 *b*. Compared to proteins of the same nominal molecular weight, the dextran molecules exhibited slower diffusion coefficients. Also shown in Fig. 2 *b* are the data published by Granath and Kvist (1967) for a set of fractionated dextrans. The empirical equations that describe the two sets of data are plotted on the same graph.

Effect of path length

Two series of experiments were performed to investigate the feasibility of using FRAP to measure diffusion in thick, scattering media. The first set of experiments examined samples of a comparatively weakly scattering agarose gel. Then, to truly test the performance of the analytical methods, a second set of experiments examined a highly scattering material with an optical density comparable to that of living tissue. The video images were analyzed by both the SFA and conventional (Chary and Jain, 1989; Kaufman and Jain, 1991) DPA methods. Two variations of the DPA method were employed: an "uncorrected" one in which the bleached spot radius was measured from the image and a "corrected" one in which the spot radius was fixed equal to the value measured in an aqueous (nonscattering) sample. The use of the smaller spot radius served as a partial correction for the error due to image distortion, but did not correct for other aspects of the distortion.

Fig. 3 summarizes the results of the FRAP measurements performed on agarose (2%) gel samples with pathlengths of 0.05 and 0.4 mm. The diffusion coefficient of FITC-Dextran (MW = 150,000) as calculated by the SFA and DPA methods are shown scaled by the diffusion coefficient measured in water (D_0). The values calculated by SFA are virtually identical ($D/D_0 = 0.71$) for the thick and thin samples ($p = 0.95$). When the same images are analyzed by the complete DPA method, the diffusion coefficients are greater ($D/D_0 = 0.86$ and 0.93 for the thin and thick pathlengths, respectively). Although there appears to be a dependence of the coefficient upon pathlength in this case, the difference is not statistically significant ($p = 0.22$). The bleached spot size as

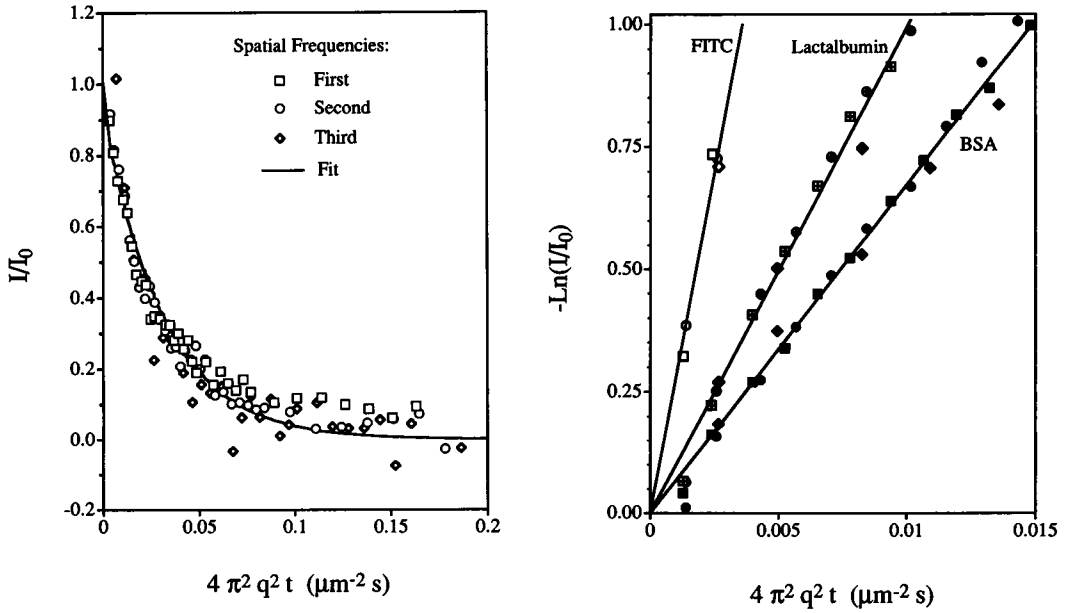

FIGURE 1 The Fourier coefficients in successive images are plotted as a function of frequency-scaled time. Components corresponding to the three lowest spatial frequencies are designated by separate symbols in order of increasing magnitude: (*square, circle, diamond*). (*a*) decay of components for BSA in aqueous solution. (*b*) decays are shown on a semilogarithmic scale for FITC (*open symbols*), lactalbumin (*crossed symbols*), and BSA (*filled symbols*) in aqueous solutions.

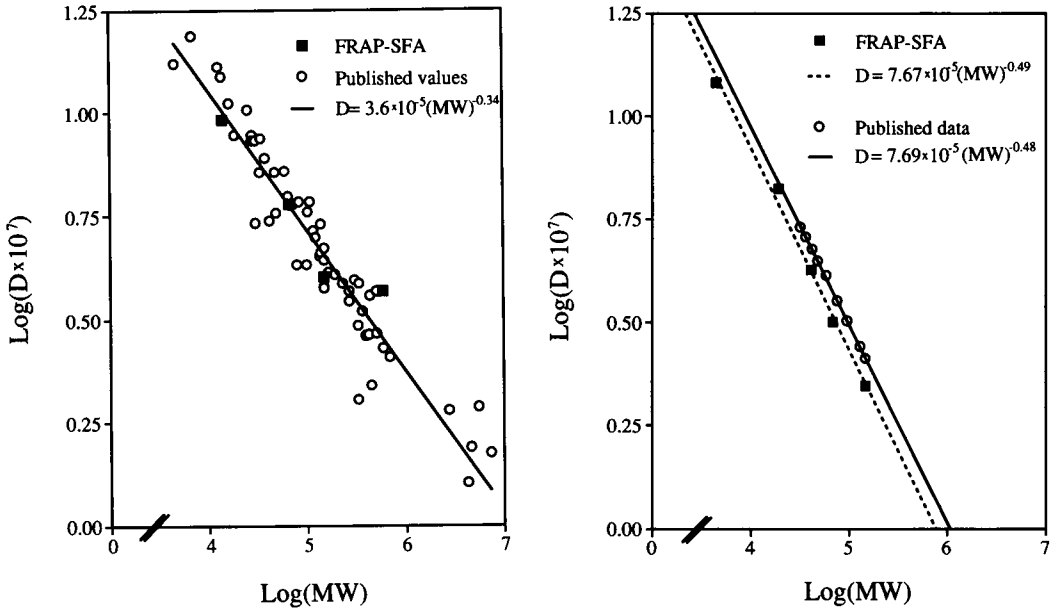

FIGURE 2 (*a*) Protein diffusion coefficients as a function of molecular weight. Values determined by FRAP with spatial Fourier analysis (*squares*) are compared with values published by various investigators (*circles*) (compiled by Altman and Dittmer, 1972). (*b*) Dextran diffusion coefficients as a function of molecular weight. Values determined by FRAP with spatial Fourier analysis (*squares*) are compared with values published by other investigators (*circles*) (Granath and Kvist, 1967).

measured from the image was apparently greater in the thick samples. The average radius was 28.8 μm for a 0.05-mm pathlength and 36.4 for a 0.4-mm pathlength. Consequently, when the same data are analyzed using the corrected DPA with a single assumed radius of 24 μm, the calculated coefficients are significantly different ($p = 0.0002$) depending on the pathlength.

In the second set of measurements, a suspension of cancer cells (45% by volume) and red blood cells (approximately 5% by volume) in an agarose gel (1 g/100 ml) was used to simulate a highly scattering, light-absorbing medium similar to tissue. FRAP measurements were performed to determine the diffusion coefficient of F-BSA in samples of various thicknesses (pathlengths of 0.2 and 0.4 mm). FRAP measurements were also performed on a "reference" sample of agarose gel without cells (pathlength 0.2 mm). Fig. 4 summarizes the results from a series of 45 recovery measurements. Diffusion coefficients are scaled by the diffusion coefficient of BSA measured in water. All methods of analysis give a comparable result for the diffusion coefficient of F-BSA in the pure gel sample with no cells ($D/D_0 = 0.65$ to 0.70); however, for the simulated tissue samples, the diffusion coefficient calculated by DPA is obviously erroneous. Both variations of the DPA give diffusion coefficients in the simulated tissue that are significantly greater than the values calculated for the reference gel ($p < 0.0001$). In fact DPA consistently gave diffusion coefficients greater than the value in water alone. When the spot radius is constrained to the value measured in a purely aqueous medium, the values calculated by the DPA method are somewhat closer to the reference value, but still several-fold greater than physically possible. Because the values of D/D_0 are so large, the results are displayed on a logarithmic scale in Fig. 4. In contrast, the diffusion coefficients in all samples calculated from the same images by SFA are less than the value in water. The mean value of D/D_0 was calculated to be 0.75 and 0.93 for the 0.2- and 0.4-mm pathlengths. The effect of pathlength is statistically significant ($p = 0.004$), but the magnitude of the effect (15% and 43% error) is not as extreme as in the case of DPA.

DISCUSSION

The results of this in vitro study validate the use of SFA for FRAP. Measured values of D in aqueous samples were comparable with published values of macromolecular diffusion coefficients as measured by various independent techniques (Altman and Dittmer, 1972; Granath and Kvist, 1967; Raj and Flygare, 1974). The results also demonstrate the reliability and accuracy of this method when the sample is thick with light-absorbing and light-scattering characteristics.

The decay of the Fourier coefficients is well described by Eq. 4. The diffusion coefficient associated with a particular fluorescence recovery was determined by a nonlinear least-squares curve fit. The error in the parameter D can be expressed as a standard deviation, based on the assumption that the error in each Fourier coefficient is normally distributed (Marquardt, 1963). The standard deviation for D in a single recovery is typically less than 5% for these in vitro experiments. When the data are plotted on a semilogarithmic scale as in Fig. 1 *b*, the linear fit has an R^2 value of greater than 95% except for the very rapid recovery corresponding to diffusion of small molecules such as FITC ($D > 20 \times 10^{-7}$ cm^2/s). For such rapid recoveries, the temporal resolution of

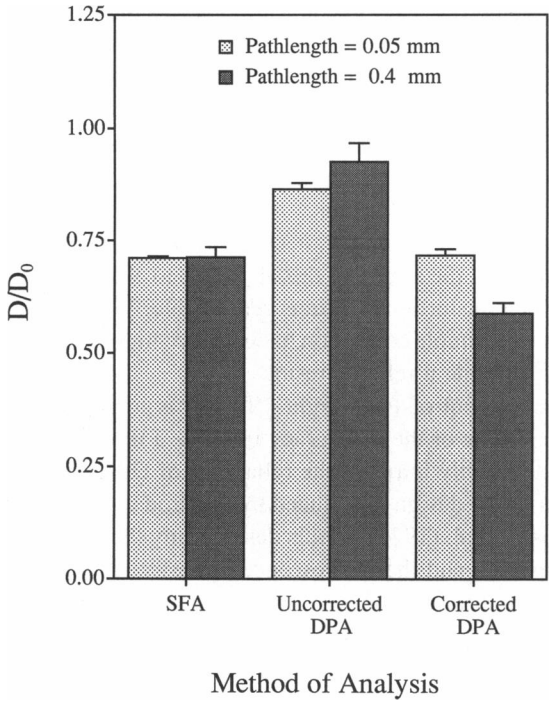

FIGURE 3 Diffusion coefficient of FITC-Dextran (MW = 150,000) in 2% agarose gel as measured in samples with pathlength 0.05 mm (*light bar*) and 0.4 mm (*dark bar*). The graph shows a comparison of results obtained by spatial Fourier analysis (SFA) and by direct photometric analysis (DPA) applied to the same video-FRAP data. In uncorrected DPA, the spot radius is measured directly from the image; in corrected DPA spot radius was measured separately in a nonscattering sample with a pathlength of 0.05 mm. Error bars show the SEM.

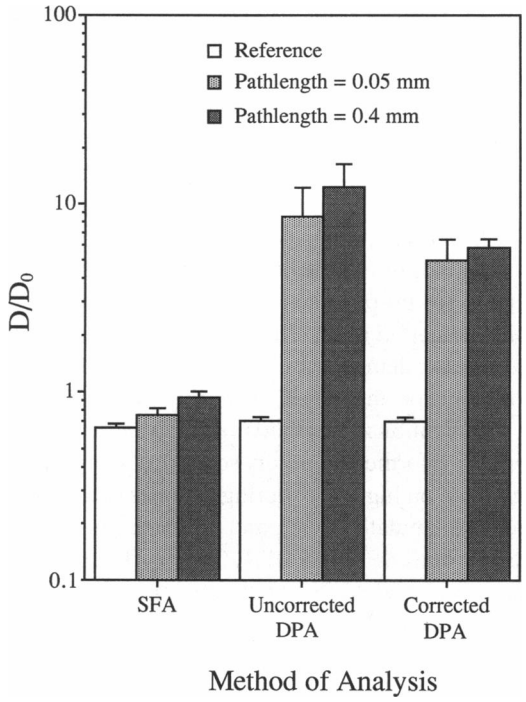

FIGURE 4 Diffusion coefficient of F-BSA in a cell-agarose composite and in a reference sample of agarose gel. The reference sample pathlength was 0.2 mm (*white bar*); the composite sample pathlengths were 0.2 mm (*light gray*) and 0.4 mm (*dark gray*). Error bars show the SEM.

the system described here is inadequate. This could be remedied by using a lower power objective to obtain a larger photobleached spot and thus increase the recovery timescale; however, the system described here is well suited to measure accurately the diffusion coefficients of macromolecules in solution and in gel matrices.

Some of the recoveries observed for the dextrans exhibited some departure from the monoexponential curve. This is attributable to the polydisperse nature of the diffusing population. The dextrans used in these experiments were claimed to possess a ratio of weight-averaged to number-averaged molecular weight of M_W:M_N < 1.2. The diffusion coefficient determined by this FRAP technique is an average, but it is not clear how this average is related to the distribution of molecular weights in the sample.

One potential source of error in the application of the SFA is the possibility of sampling error associated with the discrete Fourier transform. Sampling error occurs when the photobleached spot is not entirely contained within the acquired image. The initial photobleached spot size is smaller than the digitized image that is acquired and stored for analysis (the spot diameter is approximately half the width of the image), but diffusion causes a Gaussian spot to enlarge according to the equation given by Jain et al. (1990):

$$R^2 = R_0^2 + 8Dt \qquad (6)$$

therefore after an interval of ($t = 3R_0^2/8D$), the full 2-dimensional "waveform" that is being sampled may exceed the size of the image. When the discrete transform is performed on only a part of the waveform, sampling error may cause the discrete transform to be an inaccurate representation of the true Fourier transform (Brigham, 1974). When this criterion ($Dt < 3R_0^2/8$) is combined with Eq. 4, it can be seen that this sampling error could be a problem when:

$$-\ln (I/I_0) \geq 1.5\pi^2 q^2 R_0^2 \approx 1. \qquad (7)$$

For the system used in these experiments, the Fourier coefficients of lowest frequency ($q \approx 1/80\ \mu m^{-1}$) will decay to $1/e$ of the initial value before a sampling problem could be suspected. If there is a need to examine the later stages of recovery in more detail (for instance, to detect multiple components with different D values) then the useful range of the recovery could be extended by reducing the initial spot size relative to the image acquisition region.

The results summarized in Fig. 2 demonstrate that the FRAP technique with SFA accurately determines D for dilute aqueous solutions. The free diffusion coefficients of proteins are consistent with published values for proteins of the same molecular weight. The value obtained for BSA ($6.0 \pm 0.3 \times 10^{-7}$ cm^2/s at 23°C) is 7% lower than the value ($6.0 \pm 0.1 \times 10^{-7}$ cm^2/s, at 20°C) reported by Raj and Flygare (1974) when corrected for temperature.

It is notable that the diffusion coefficients of the dextrans are significantly lower than the coefficients for proteins of the same molecular weight. This phenomenon can be attributed to a configurational effect: dextran is a linear flexible

polymer unlike most proteins. This is further demonstrated by the molecular weight dependence for the diffusivities of the two classes of molecules. The logarithmic plot in Fig. 2 *a* reveals that protein aqueous diffusion coefficients are approximately proportional to molecular weight to the −1/3 power. This is consistent with the Stokes-Einstein equation for diffusivity with the assumption that the molecule is a sphere with volume proportional to its molecular weight. On the other hand, Fig. 2 *b* demonstrates that dextran diffusion coefficients are proportional to the −1/2 power.

The investigation of the effect of pathlength, summarized in Figs. 3 and 4, demonstrates the superiority of SFA for the study of diffusion in a thick, scattering medium, compared to two "conventional" methods of analysis. FRAP experiments were performed on mildly scattering samples (agarose gel alone) and on highly scattering samples (cells suspended in agarose to simulate tissue), and the same image data were analyzed by both SFA and DPA. The coefficient calculated by SFA is independent of sample thickness for mildly scattering media, and only moderately dependent on pathlength in highly scattering media. In contrast, the DPA method of analysis can show a pathlength dependence even under mild scattering conditions and is completely untenable for thick, optically dense media.

The results of the FRAP experiments conducted upon the agarose gel samples, summarized in Fig. 3, illustrate the sensitivity of direct photometric analysis to the dimension of the bleached spot. The "uncorrected" DPA gives a value of $D/D_0 = 0.9$, independent of pathlength. However, this value is higher than previously reported values of restricted diffusion. Ackers and Steere (1962) reported $D/D_0 = 0.6$ to 0.7 for the restricted diffusion of BSA and IgG in 2% agar gel, and Moussaoui et al. (1992) reported a value of $D/D_0 \approx 0.7$ for the diffusion of BSA and ovalbumin in 2% agarose beads. Thus the value of $D/D_0 = 0.71$ obtained by SFA appears to be more accurate than the DPA result. When the spot radius is assumed to be 24 μm, the radius measured in a thin aqueous sample, the corrected DPA result for short pathlength (0.05 mm) is consistent with the SFA result. However, when this corrected DPA is applied to the long pathlength (0.4 mm) samples, the calculated coefficients are significantly lower. It can be concluded that in a light-scattering sample the bleached spot radius is not independent of sample thickness but that the observed spot radius will be larger than the true radius. Given the sensitivity of the calculation to R_0, it will be difficult to select a reliable R_0 value to be used in DPA.

The failure of DPA is only partially related to the distortion that makes the spot radius appear larger than the true photobleached region. The experiments with the cell suspension, summarized in Fig. 4, show that there is another optical phenomenon associated with a strongly scattering material that causes a rapid fluorescence recovery. A spot radius of less than 10 μm would have to be assumed in order to calculate a realistic diffusion coefficient by the DPA method. It is unlikely that the sample could somehow reduce the spot radius to less than the Gaussian radius of the laser intensity pattern. An examination of the images shows that much of the rapid recovery occurs uniformly across the field of view. Therefore it is likely that this recovery represents the contribution of out-of-focus or diffusely scattered light. In the Fourier transform space this rapid recovery affects primarily the zero frequency component rather than the non-zero frequencies that are used in SFA; hence, the SFA method is more resistant to this artifact. Although the SFA results from the simulated tissue experiments do exhibit some pathlength dependence, the ability of this approach to eliminate most of the image distortion effects is remarkable. We were unable to devise a simple correction to our conventional method that would provide a reliable result.

Because out-of-focus light ("flare") is implicated as the major source of the inaccuracy in DPA, a modification that would possibly improve the reliability of DPA would be to return to the design introduced by Axelrod et al. (1976) and Jacobson et al. (1976). In this design, only the spot region is illuminated, and the fluorescence intensity is monitored by a photomultiplier tube with an aperture to eliminate out-of-focus light. This arrangement eliminates much of the scattered light via a confocal effect. The disadvantage of this approach is the loss of spatial information that is obtained with the image analysis approach. With the photomultiplier approach, it is difficult to simultaneously detect and measure convective velocity or anisotropic diffusion. It is also not clear whether the confocal effect would be sufficient to remove enough of the scattered light when the spot radius is relatively large (~20 μm). Finally, the uncertainty regarding the true spot size in the thick sample may remain.

The data confirm our finding that for tumor tissue of thickness 0.5 to 2 mm, the conventional direct photometric analysis of the FRAP experiment can lead to inaccurate measurements of D. The cell-agarose composite created for these experiments is a light-scattering, light-absorbing medium that strongly degrades the microscopic image; it is unlikely that actual tissue would present a more demanding medium. These gel composite experiments demonstrate that the use of SFA with FRAP can provide measurements of diffusion coefficient that are relatively insensitive to sample thickness, and the experiments in aqueous media show that the accuracy of the method is comparable to that of our conventional approach (i.e., DPA). Based on these results, SFA is the best available method for obtaining a reliable measure of the interstitial diffusion coefficient in most tissues.

For detection of simultaneous convection, the previously published method of tracking the movement of the spot center remains reliable because it does not depend on the exact correspondence of intensity with concentration. As pointed out by Tsay and Jacobson (1991), convection can also be detected in the Fourier transform space by examining the change in phase in the complex coefficients. In these experiments, in which there was no convection or translation of the sample, the phase did not change over the course of the recovery. Another positive aspect of the SFA for diffusion measurement is that motion of the spot (due to convection or due to motion of the sample) does not affect the

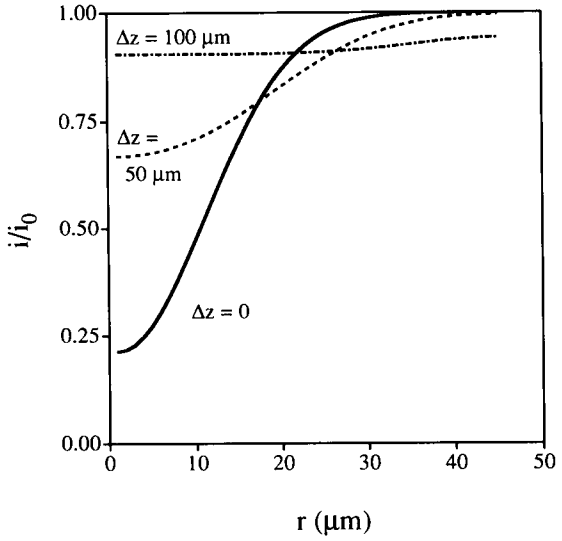

FIGURE 5 Theoretical fluorescence image intensity of a Gaussian bleached spot on a thin membrane. The spot is viewed through a microscope (20×, 0.40 N.A. objective) at different levels of defocus. The apparent spot profile becomes broader and shallower as the distance (Δz, in μm) between the membrane and the focal plane increases.

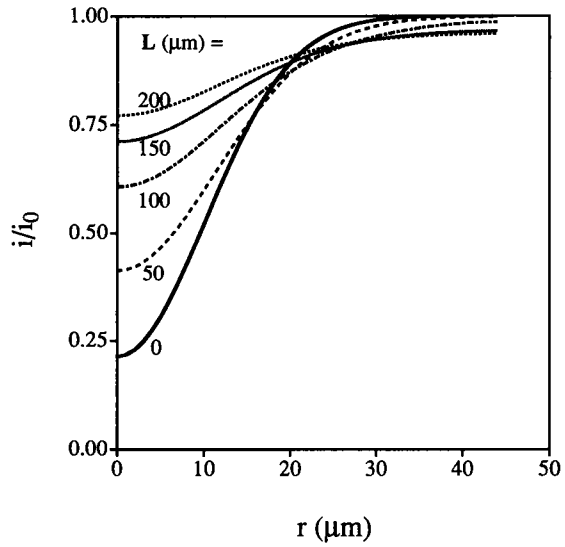

FIGURE 6 Theoretical fluorescence image intensity of a Gaussian bleached spot in a thick, uniform sample, viewed through the microscope (20×, 0.40 N.A. objective). The top of the sample coincides with the focal plane. As sample thickness (L, in μm) increases, the apparent spot profile becomes broader and shallower. Effects of light scattering and absorption are not incorporated into the theoretical model.

amplitude of the Fourier coefficients. Of course this insensitivity to motion only applies if the spot remains inside the sampling region.

Another advantage of the SFA is its potential for the detection of anisotropic diffusion. This feature was discussed by Tsay and Jacobson (1991). This feature could be useful in future studies that might seek to correlate structural features with anisotropic diffusion in tissue.

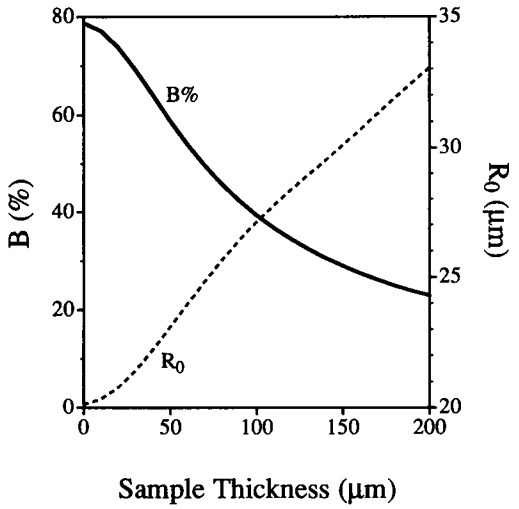

FIGURE 7 Effect of sample thickness on apparent spot radius (R_0) and depth of bleach ($B\%$). The theoretical calculation is based upon the simulations shown in Fig. 6.

APPENDIX

This section uses the theory of image formation (Castleman, 1979; Agard, 1984) to describe how the fluorescence image of a bleached spot is distorted by the out-of-focus light and how the distortion will affect the measurement of diffusion coefficient in thick samples (>50 μm) using a conventional FRAP method such as that used by Jain et al. (1990). To simplify the analysis, we did not consider the light scattering and absorption in the sample. Therefore the analysis generated represents the best possible resolution of fluorescence distribution for a given objective.

In order to determine what degree of distortion to expect from the microscope system and whether that distortion could affect the FRAP results, a series of images were constructed based on theoretical formulations of the fluorophore concentration distribution and the microscope optical characteristics (OTF). We use in this analysis the theoretical OTF derived by Stokseth (1969) and modified by Agard (1984) for an objective with a given numerical aperture (N.A. = 0.4), focal length (d_f = 10.1 mm) and the extent of defocus (Δz).

$$\mathrm{OTF}(q) = (1 - 0.696b + 0.000766b^2 + 0.0436b^3)g\left[\frac{4\pi w}{\lambda}(2 - b)b\right] \quad \text{(A1)}$$

where

$$w = -d_f - \Delta z \cos\alpha + (d_f^2 + 2d_f\Delta z + \Delta z^2\cos^2\alpha)^{1/2}$$

$$g(x) = 2\frac{J_1(x)}{x}, \quad b = \frac{2q}{f_c}, \quad f_c = 2\frac{\text{N.A.}}{\lambda},$$

$$\cos\alpha = \sqrt{1 - \text{N.A.}^2}, \quad q = \sqrt{u^2 + v^2}$$

u and v are the spatial frequencies of Fourier transform, λ is the wavelength (515 nm), $J_1(x)$ is the first-order Bessel function, and the objective is assumed to be "dry" (refractive index between objective and sample is equal to 1).

The fluorescence profile was first calculated for a two-dimensional spot (an infinitely thin sample) when the spot is focused ($\Delta z = 0$) and for various distances (Δz) out of focus. The results of simulations are shown in Fig. 5. The concentration of fluorescent molecules was assumed to follow a Gaussian profile such as would be created by a nondiverging laser beam passing through the sample. When the thin sample is in focus, the image is a good (but not perfect) representation of the concentration distribution, and the distortion increases as the two-dimensional object moves farther out of fo-

cus. It is evident from the figure that as the object moves farther out of focus, the apparent spot radius increases and the apparent depth of the bleach decreases.

A thick sample (>50 μm) can be regarded as a stack of very thin planes such that only one plane is truly in focus. Each plane of the sample has the same concentration distribution of fluorescent molecule and contributes to the observed image; thus, the out-of-focus components may cause significant distortion. Fig. 6 illustrates how the observed fluorescence profile may vary with sample thickness (L). Fig. 7 illustrates how the apparent depth of the bleach and the apparent spot radius change as sample thickness increases. The apparent bleached spot is shallower and larger than the true concentration profile. As both the bleach depth and spot radius are important parameters in the calculation of the diffusion coefficient (Jain et al., 1990), thick-sample distortion could lead to inaccurate results. For example, the depth of the bleach (B) and the radius of the spot (R_0) are related to the diffusion coefficient (D) according to the equation:

$$B/B_0 = [1 + 8Dt/R_0^2]^{-1} \quad \text{(A2)}$$

Although the errors in bleach depth may cancel to some extent, the amplification of the apparent spot size (R_0) will lead to an overestimation of D.

We thank Drs. Eric Kaufman, Robert Melder, and Richard Stock for assistance in setting up the microscope and image processing system, and Dr. Leo Gerweck for providing tumor cells and excellent advice on formulating the simulated tissue samples.

This work was supported by a grant from the National Cancer Institute CA56591 to R. K. J., by a National Research Service Award CA59255 to D. B., and by a Feodor Lynen Fellowship from the Humboldt Foundation to M. L.

REFERENCES

Ackers, G. K., and R. L. Steere. 1962. Restricted diffusion of macromolecules through agar-gel membranes. *Biochim. Biophys. Acta.* 59:137–149.

Agard, D. A. 1984. Optical sectioning microscopy: cellular architecture in three dimensions. *Annu. Rev. Biophys. Bioeng.* 13:191–219.

Altman, P. L., and D. S. Dittmer. 1972. Biology Data Book. Federation of American Societies for Experimental Biology, Bethesda, MD. 370–385.

Axelrod, D., D. E. Koppel, J. Schlessinger, E. Elson, and W. W. Webb. 1976. Mobility measurement by analysis of fluorescence photobleaching recovery kinetics. *Biophys. J.* 16:1055–1069.

Brigham, E. O. 1974. The Fast Fourier Transform. Prentice-Hall, Englewood Cliffs, NJ. 91–109.

Castleman, K. R. 1979. Digital Image Processing. Prentice-Hall, Englewood Cliffs, NJ.

Chary, S. R., and R. K. Jain. 1989. Direct measurement of interstitial convection and diffusion of albumin in normal and neoplastic tissues by fluorescence photobleaching. *Proc. Natl. Acad. Sci. USA.* 86:5385–5389.

Clauss, M. A., and R. K. Jain. 1990. Interstitial transport of rabbit and sheep antibodies in normal and neoplastic tissues. *Cancer Res.* 50:3487–3492.

Granath, K. A., and B. E. Kvist. 1967. Molecular weight distribution analysis by gel chromatography on Sephadex. *J. Chromatogr.* 28:69–81.

Hiraoka, Y., J. W. Sedat, and D. A. Agard. 1990. Determination of three-dimensional imaging properties of a light microscope system: partial confocal behavior in epifluorescence microscopy. *Biophys. J.* 57:325–333.

Hopkins, H. H. 1955. The frequency response of a defocused optical system. *Proc. R. Soc. (Lond.).* A231:91–103.

Jain, R. K. 1987. Transport of molecules in the tumor interstitium: a review. *Cancer Res.* 47:3039–3051.

Jain, R. K. 1993. Physiological resistance to the treatment of solid tumors. *In* Drug Resistance in Oncology. B. A. Teicher, editor. Marcel Dekker, Inc., New York. 87–105.

Jain, R. K., and L. T. Baxter. 1988. Mechanisms of heterogeneous distribution of monoclonal antibodies and other macromolecules in tumors: significance of elevated interstitial pressure. *Cancer Res.* 48:7022–7032.

Jain, R. K., R. J. Stock, S. R. Chary, and M. Rueter. 1990. Convection and diffusion measurements using fluorescence recovery after photobleaching and video image analysis: In vitro calibration and assessment. *Microvasc. Res.* 39:77–93.

Fox, J. R., and H. Wayland. 1979. Interstitial diffusion of macromolecules in the rat mesentery. *Microvasc. Res.* 18:255–276.

Jacobson, K. A., Z. Derzko, E.-S. Wu, Y. Hou, and G. Poste. 1976. Measurement of the lateral mobility of cell surface components in single, living cells by fluorescence recovery after photobleaching. *J. Supramol. Struct.* 5:565–576.

Kaufman, E. N., and R. K. Jain. 1991. Measurement of mass transport and reaction parameters in bulk solution using photobleaching: reaction limited binding regime. *Biophys. J.* 60:596–610.

Lanni, F., D. L. Taylor, and B. R. Ware. 1981. Fluorescence photobleaching recovery in solutions of labeled actin. *Biophys. J.* 35:351–364.

Laurent, T. C., I. Björk, A. Pietruszkiewicz, and H. Persson. 1963. On the interaction between polysaccharides and other macromolecules. *Biochim. Biophys. Acta.* 78:351–359.

Maroudas, A. 1980. Physical chemistry of articular cartilage and the intervertebral disc. *In* The Joints and Synovial Fluid. Vol 2. L. Sokoloff, editor. Academic Press, New York. 240–293.

Marquardt, D. 1963. An algorithm for least-squares estimation of nonlinear parameters. *SIAM J. Appl. Math.* 11:431–441.

Moussaoui, M., M. Benlyas, and P. Wahl. 1992. Diffusion of proteins in Sepharose Cl-B gels. *J. Chromatogr.* 591:115–120.

Nakamura, Y., and H. Wayland. 1975. Macromolecular transport in the cat mesentery. *Microvasc. Res.* 9:1–21.

Nugent, L. J., and R. K. Jain. 1984. Extravascular diffusion in normal and neoplastic tissues. *Cancer Res.* 44:238–244.

Ogston, A. G., B. N. Preston, and J. D. Wells. 1973. On the transport of compact particles through solutions of chain polymers. *Proc. R. Soc. (Lond.).* A333:297–309.

Peters, R., J. Peters, K. H. Tews, and W. Bahr. 1974. A microfluorometric study of translational diffusion in erythrocyte membranes. *Biochim. Biophys. Acta.* 367:282–294.

Raj, R., and W. M. Flygare. 1974. Diffusion studies of bovine serum albumin by quasielastic light scattering. *Biochemistry.* 13:3336–3340.

Stokseth, P. A. 1969. Properties of a defocused optical system. *J. Opt. Soc. Am.* 59:1314–1321.

Tanke, H. J., P. Van Oostveldt, and P. Van Duijn. 1982. A parameter for the distribution of fluorophores in cells derived from measurements of innerfilter effect and reabsorption phenomenon. *Cytometry.* 6:359–369.

Tsay, T-T., and K. A. Jacobson. 1991. Spatial Fourier analysis of video photobleaching measurements: principles and optimization. *Biophys. J.* 60:360–368.

Yguerabide, J., J. A. Schmidt, and E. E. Yguerabide. 1982. Lateral mobility in membranes as detected by fluorescence recovery after photobleaching. *Biophys. J.* 39:69–75.